Solar wind and Sunspot variability in the 23rd and 24th solar cycles: A comparative analysis

M. Adhikary[1] and P.K. Panigrahi[2]

[1] 2nd year MS (Physical Science), Department of Applied Sciences, Gauhati University, Guwahati-781014, India.
[2]Department of Physical Sciences, Indian Institute of Science Education and Research, Kolkata, Mohanpur-741246, India
Email: [1]adhikary.manashee@gmail.com , [2]pprasanta@iiserkol.ac.in

Abstract: A comparative analysis of the stationary and non-stationary periodic variations of sunspot number and the solar wind flow speed is carried out for the 23rd and the 24th solar cycles. The variations of the sunspot number and solar wind speed at one AU distance from the Sun are identified through Fourier and Wavelet transforms. The former revealed significant inter and intra-cycle differences of the three dominant periodic components of durations 27, 13.5 and 9 days. The global Morlet wavelet spectra showed the stationarity of the dominant 27-day periodicity of the sunspot number and solar wind arising from Sun's rotation. The additional periodicities of 13.5-day and 9-day of the solar wind have non-stationary character, with strong intra cycle differences. Our analysis establishes correlation of topographical variation and spatial distribution of coronal holes with the fast components of the solar wind.
Keywords: Solar wind, Sunspot variability, Solar cycle, Wavelet transform

1. INTRODUCTION

Solar wind is a highly ionized magnetized plasma, originating from the Sun's corona and spread across a large volume known as the heliosphere, extending beyond the orbit of Pluto. Analysis of the periodic variations of solar wind (SW) in conjunction with the sunspot activity provides an ideal system for unravelling the dynamics of the fast and slow constituents of the solar wind and also the possible role of interplanetary medium where these two components interact. During a typical Solar cycle, darker regions known as "Sunspots" appearing from the relatively cooler regions of the solar photosphere, as a result of the periodic variation of the Solar magnetic field, pass a maximum-minimum-maximum phase in almost 11 years. The Solar wind parameters show signature of various high resolution periodicities, which can vary significantly in different cycles. In regions close to the Sun, SW consists of slow (~ 400 km/sec) and high speed (~ 750 km/sec) components, the former emanating from coronal holes and the latter possibly from the streamers [1]. During the period of a solar minima when the appearance of the Sunspots is minimal, large and stable coronal holes occur at the Sun's polar regions. They appear at lower latitudes during more active periods, which causes geomagnetic storms in the magnetosphere of Earth [2]. However, there is little understanding of the cause for the high velocity of the wind from these coronal gases [3]. Use of elemental abundances and freeze-in temperatures, as well as comparison of remote observations with in-situ properties of solar wind have been proposed for tracing the sources of these two types of SW [4] . The study of SW behaviour in the interplanetary region is important for finding out the nature of interaction between high-speed and slow-speed components that alternately pass by Earth as the Sun rotates with a time-period of 27 days. Furthermore, SW has a significant effect on the space weather, making its study an area of active research [5], [6], [7]. Solanki et al. [8] have reconstructed sunspot number covering the past 11, 400 years,

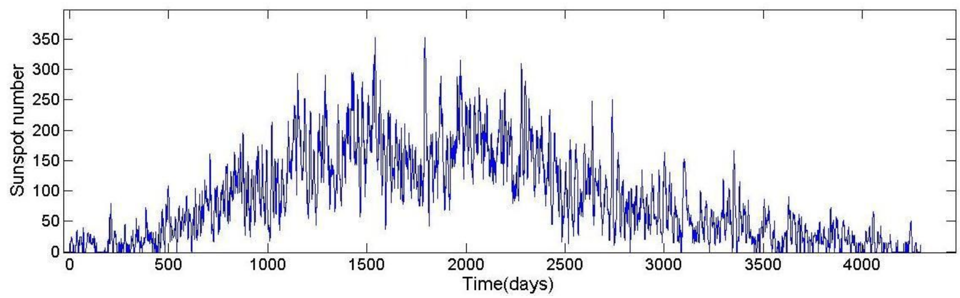

Figure 1: The daily sunspot number variation in the solar cycle 23, showing a double peak

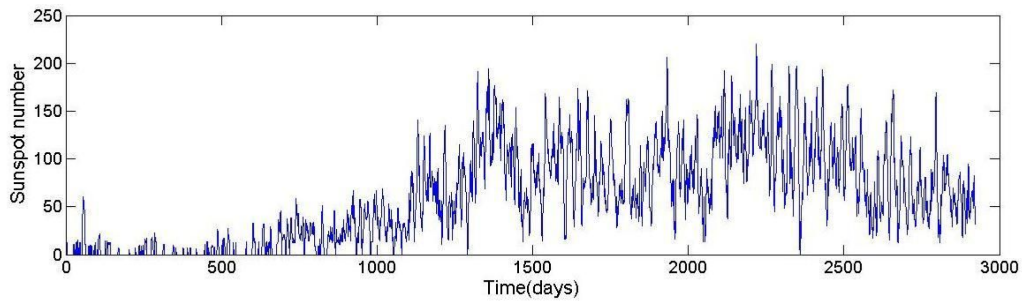

Figure 2: The daily sunspot number variation in the solar cycle 24, showing double peak structure

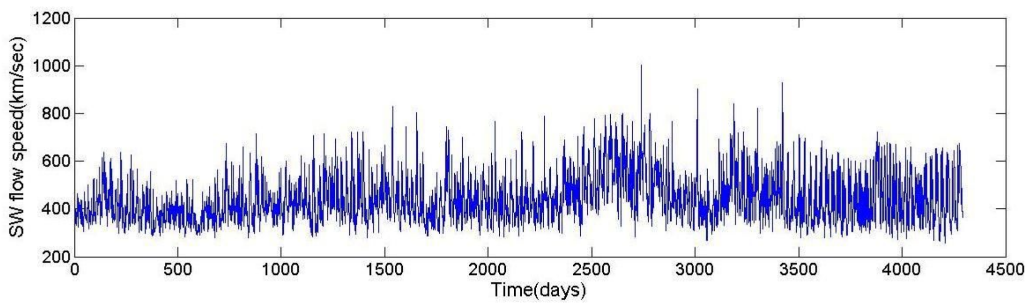

Figure 3: Time series plot of solar wind flow speed near 1 AU in the solar cycle 23

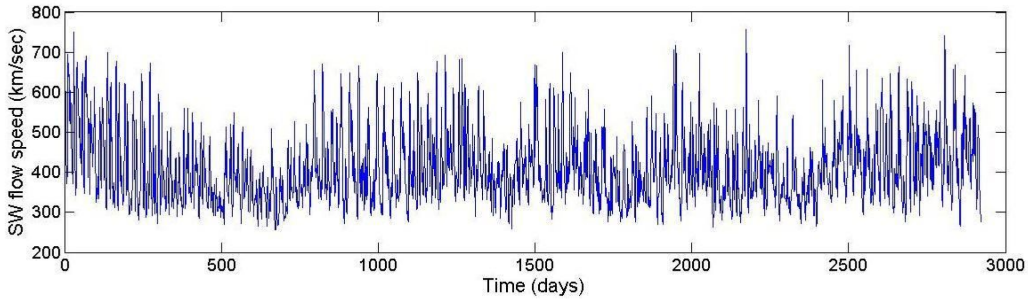

Figure 4: Time series plot of solar wind flow speed near 1 AU in the solar cycle 24

finding that the level of solar activity during the past 70 years has been exceptional. They also observed that the solar variability is unlikely to be the dominant cause for the recent unusual warming.

A recent study has showed that since mid 1990s, there has been a steady decline of the solar photospheric fields at latitudes $\geq 45^o$, as well as heliospheric microturbulence levels, [9] indicating weakening of the solar magnetic field. This is expected to affect the solar wind production and variability. The solar wind has strong impact on the terrestrial environment. Earth's thermosphere, extending about 60 to 300 miles above its surface, is constantly interacting with the solar wind. This interaction leads to density change of thermosphere that causes rise and fall of temperature, expanding and contracting on a 27-day period due to variation in extreme UV radiation. A systematic study showed that the periodic "breathing" of Earth's upper atmosphere is directly dependent on the solar wind variation [10]. It also indicated that high-speed wind from the sun triggers independent breathing episodes by creating geomagnetic disturbances. This atmosphere layer has periodic oscillation of 9 days, caused by the violent effect of the high-speed solar winds interacting with Earth's upper atmosphere. Both the sunspot activity and the SW variations are expected to vary in different cycles. The 23^{rd} solar cycle, starting from mid 1996 and ending in the beginning of 2008, was a rather long one, lasting for 11.7 years, and a quiet one too. Currently, the 24^{th} cycle is in progress since 4^{th} January, 2008, having minimal activity until early 2010. According to the current predictions and observations, it is expected to be the smallest sunspot cycle since the cycle 14.

In the following, the 23^{rd} and 24^{th} cycles are studied, based on average solar wind speed as it reaches Earth's orbit, correlating with the variability in the sunspot number. We have collected 1-day resolution data from OMNIWeb data facility of NASA's SPDF Goddard Space Flight Centre, comprising of sunspot number and the solar wind flow speed (km/sec) near 1 AU from Sun, for both the cycles. *Figure 1* and *Figure 2* show the time-series plots of sunspot number respectively for the cycle 23 and 24 whereas *Figure 3* and *Figure 4* show the SW flow speed for the 23^{rd} and 24^{th} cycle for our analysis. Fourier transform is then used to find out hidden periodicities and to compare periodic variation of solar wind with the sunspot activity, and the nature of correlation of the periodic components in the 23^{rd} and 24^{th} cycles. For identification of time-frequency localization of the periodic variations, we apply Continuous Wavelet Transform (CWT) and analyse global wavelet spectra with 95% confidence level. This shows the stationarity of the dominant periodicity and non-stationary nature of the other two variations of 13.5-day and 9-day periods.

2. FOURIER TRANSFORM ANALYSIS

Fourier transform is a convenient tool for identifying the presence of periodic behaviour in a time series [11], characterized by sharp peaks in the power spectrum. It splits a time domain signal ($f(t)$) to complex exponential functions of different frequencies [12],

$$F(\omega) = \int_{-\infty}^{\infty} f(t) e^{-i\omega t} dt$$

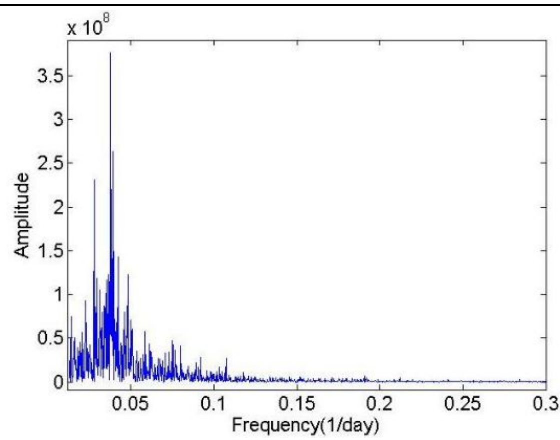

Figure 5: Fourier power spectrum of sunspot number for solar cycle 23 showing one dominant peak corresponding to 27 days

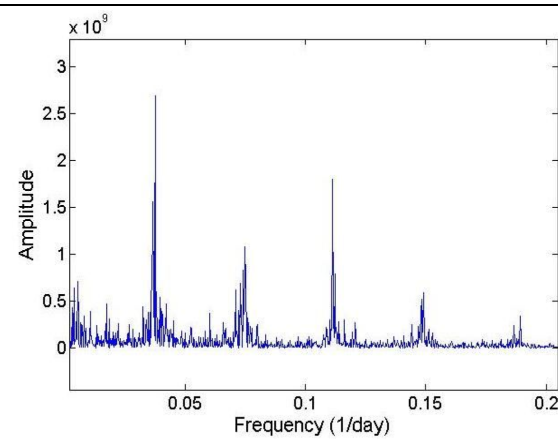

Figure 6: Fourier power spectrum of SW flow speed for solar cycle 23 showing three dominant periodic components corresponding to 27, 13.5 and 9 days

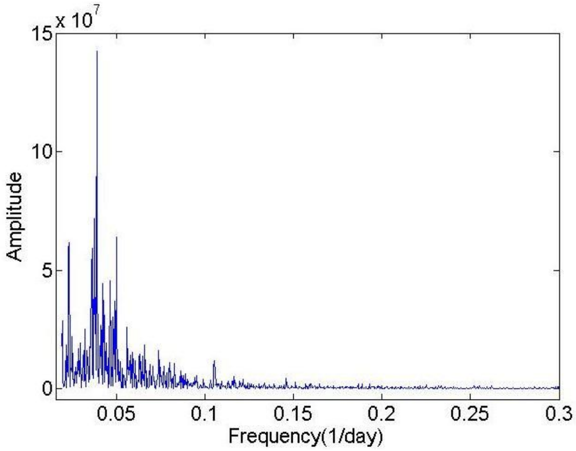

Figure 7: Fourier power spectrum of sunspot number for solar cycle 23 showing one dominant peak corresponding to 27 days

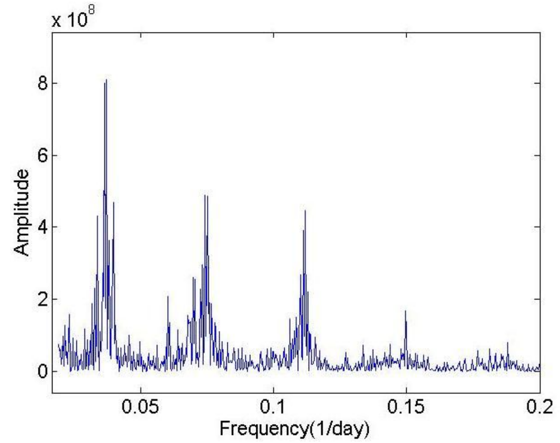

Figure 8: Fourier power spectrum of SW flow speed for solar cycle 23 showing three dominant periodic components corresponding to 27, 13.5 and 9 days

Figure 5 and *Figure 6* depict Fourier transforms of the sunspot number and SW flow speed for the cycle 23, and *Figure 7* and *Figure 8* show the same for the cycle 24. The observed periodicities of solar wind match with previous studies. Periodicities of these two parameters, i.e., sunspot number variation and solar wind speed, show significant differences in both the cycles. The 27-day periodicity of sunspot activity clearly represents the solar rotation period, while the other higher resolution periodicities of 13.5-day and 9-days arise in solar wind speed which are absent in the sunspot number. Our Fourier spectra clearly reveals periodicities, from where, comparison of amplitudes of the Fourier powers also yields interesting inferences. *Table 1* depicts amplitudes of Fourier powers for all the parameters considered for both the cycles. It can be observed that the Fourier amplitude of the 27-day periodic variation of sunspot number in 23^{rd} and 24^{th} cycles are quite comparable, implying same persistency of solar rotation period imposed on sunspot number variation. Solar wind, on the other hand, as it propagates towards earth shows signature of higher resolution periodicities of 13.5 and 9 days, with less amplitudes in case of cycle 24. Thus the 24^{th} cycle is showing less stationarity

Table 1: Fourier amplitudes and periodicities

Parameter	Periodicity (days)	Fourier power (a.u.) (cycle 23)	Fourier power (a.u.) (cycle 24)
Sunspot Number	27	3.76×10^{8}	1.42×10^{8}
SW flow speed	27	2.69×10^{9}	8.08×10^{8}
	13.5	1.07×10^{9}	4.89×10^{8}
	9	1.80×10^{9}	4.46×10^{8}

of periodic behaviour along with less activity as compared to the former cycle. The significant difference in Fourier power for the two cycles implies variation in stationarity of the periodic modulations in SW speed. We therefore apply Continuous Wavelet Transform (CWT) for the visualization of time-frequency localization of these components, which is described in detail in the following section.

3. WAVELET TRANSFORM ANALYSIS

Wavelet transform may be considered as a mathematical microscope that reveals the behaviour of the signal in both time and frequency domain [13], [14]. This has to be compared with the Fourier transform, popularly called the 'mathematical prism', which reveals either the frequency or time variations. The "wavelet" is a small wave that has an oscillating wavelike characteristic and has its energy concentrated in time. Wavelet Transform (WT) makes it possible to use variable window sizes in analysing different frequency components within a signal or a time series, which is not permitted in case of Fourier Transform or even Short time Fourier Transform (STFT). When the given signal is compared with a set of functions obtained from the scaling and shift of a base wavelet, say "Morlet", the analysis is realized as shown in *Figure 9* [15].

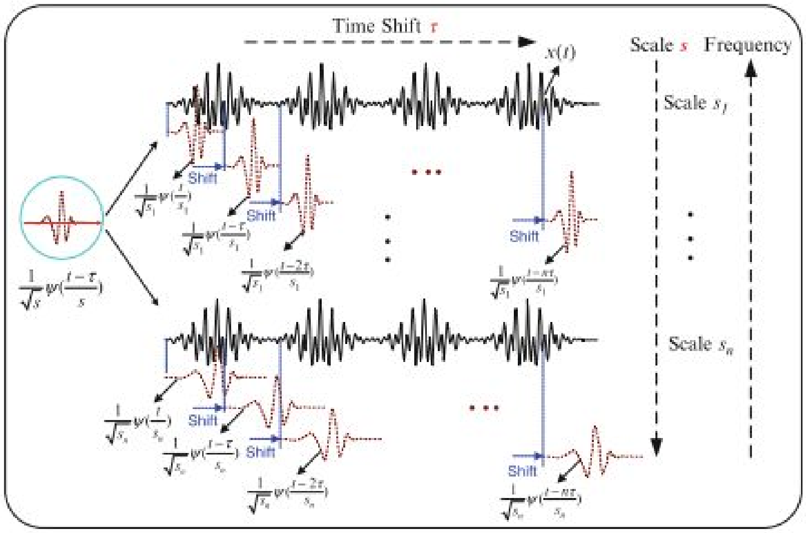

Figure 9: Wavelet Transform: enabling time-frequency analysis through different windows by scaling and shifting a base wavelet

Mathematically, Wavelet Transform (WT) can be expressed as

$$wt(s.\tau) = \langle x, \Psi_{s,\tau} \rangle = \frac{1}{\sqrt{s}} \int_{-\infty}^{\infty} x(t)\Psi^*(\frac{t-\tau}{s})dt$$

and the variations of the time and frequency resolutions of the base wavelet, taken as Morlet wavelet here, at two locations on the time–frequency plane, (τ_1, η/s_1) and (τ_2, η/s_2) are depicted in the *Figure 10* [15].

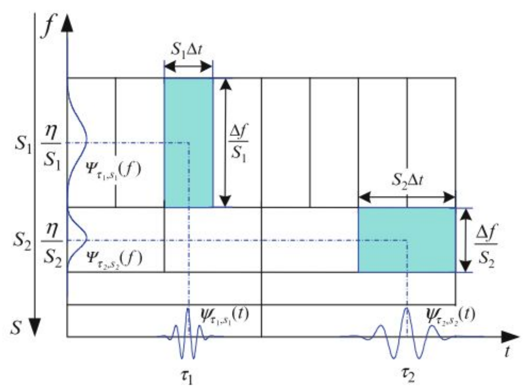

Figure 10: Variation of Morlet Wavelet in the time-frequency plane

By executing variations of the scale and time shifts of the base wavelet function intelligently, the WT can be used very effectively to extract the frequency components over the entire spectrum, by using small scales for decomposing high frequency parts and large scales for analysing the low frequency components.

The definition of the Continuous Wavelet Transform (CWT) may be found as

$$X(a,b) = \frac{1}{\sqrt{b}} \int_{-\infty}^{\infty} x(t)\Psi\left(\frac{t-a}{b}\right)dt$$

where 'a' shifts time, 'b' modulates the width (and not the frequency), and $\Psi(t)$ is the mother wavelt, which is taken as Morlet in the present work [16]. Morlet is a Gaussian windowed wavelet with sinusoidal modulations:

$$\psi_0(t) = \pi^{-\frac{1}{4}} e^{i\omega_0 t} e^{-\frac{1}{2}t^2}$$

Here, 'ω_0' is dimensionless frequency and 't' is dimensionless time. The wavelet coefficients $C_{a,b}$ are then obtained from the convolution of data $f(t)$ with the wavelet $\Psi(t)$ as defined above, to come up with the net WT of the entire time series as a superposition of WT obtained from different windows used for the analysis. The dominant frequency components in the time series, at a particular instant of evolution, may thus be pinpointed by finding a higher value of this wavelet coefficient.

Figure 11 and *Figure 12* show CWT periodograms (global wavelet spectrum) of sunspot number and wind flow speed of cycle 23 and *Figure 13* and *Figure 14* show the same for cycle 24. While the x- and y- axes denote the time progression of the series and the scales used for localizing the analysis on the time-frequency plane, the magnitude of the wavelet coefficients is defined by the colour plot along the z-axis, red denoting highest and blue denoting lowest. The persistency of periodicities present in both the cycles can be clearly seen in this localized time-frequency plane analysis.

The 27-day periodicity is observed throughout the 11-year cycle of sunspot activity, whereas it is less stationary in flow speed along with additional 13.5-day and 9-day periodicities. The wavelet spectrum of solar wind speed in the 23rd cycle reveals that the 13.5-day periodicity is present in the declining phase when the Sunspot number comes down gradually from the Solar maximum.

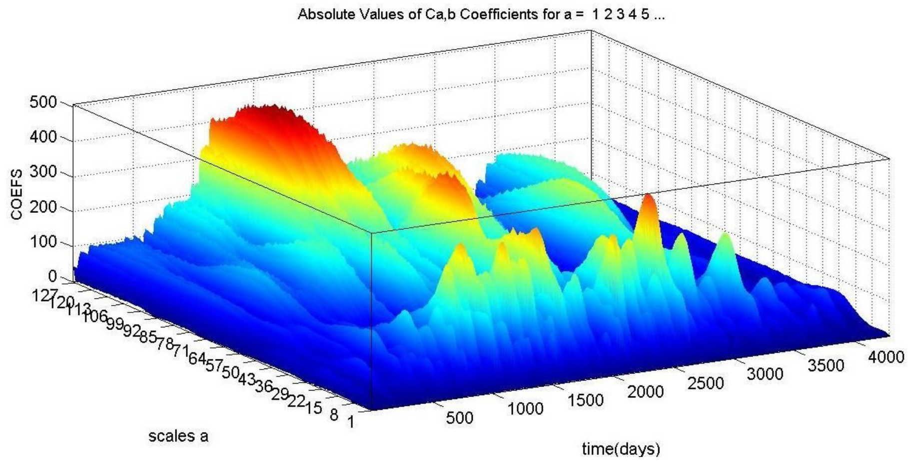

Figure 11: CWT periodogram of daily sunspot number for solar cycle 23, revealing stationary periodic variations corresponding to 27 days, while low frequency stationary noise too shows up during Solar maxima (middle portion)

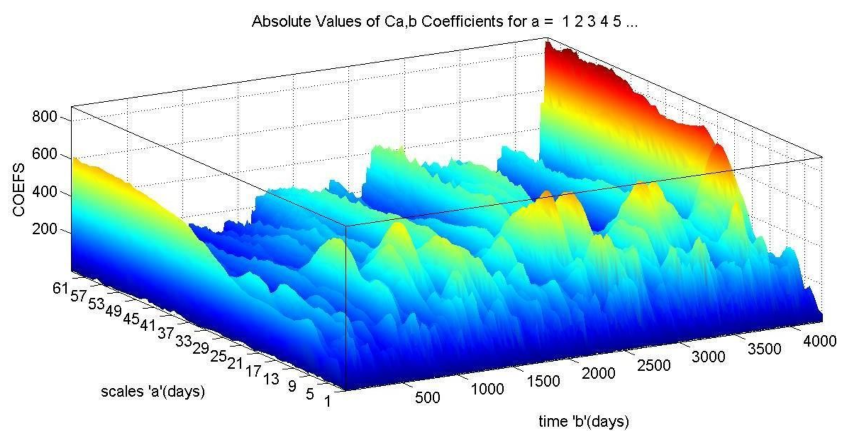

Figure 12: CWT periodogram of SW flow speed for solar cycle 23, revealing stationary and non-stationary periodic variations corresponding to 27, 13.5 and 9 days, while low frequency noise shows up during Solar minima (end portions)

The interaction of large-scale solar magnetic fields with the solar plasma leads to formation of coronal holes on the solar corona. These holes are said to have unipolar magnetic fields that open freely into the interplanetary medium, pushing fast streams of solar wind. During a solar cycle, coronal holes cover the polar regions during minimum activity, while they are distributed throughout all solar latitudes during more active periods, with less stability. Also, the coronal holes are more noticeable in the declining phase of the solar cycle [17].

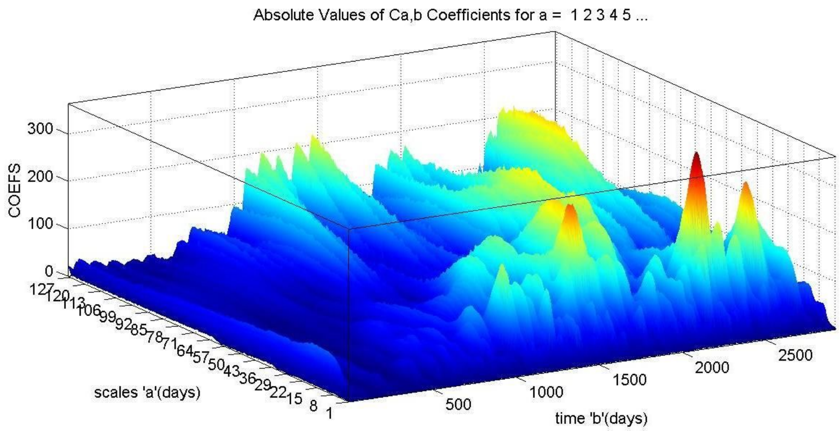

Figure 13: CWT periodogram of daily sunspot number for solar cycle 24, revealing stationary periodic variations corresponding to 27 days, while low frequency non-stationary noise shows up during Solar minima-maxima phase

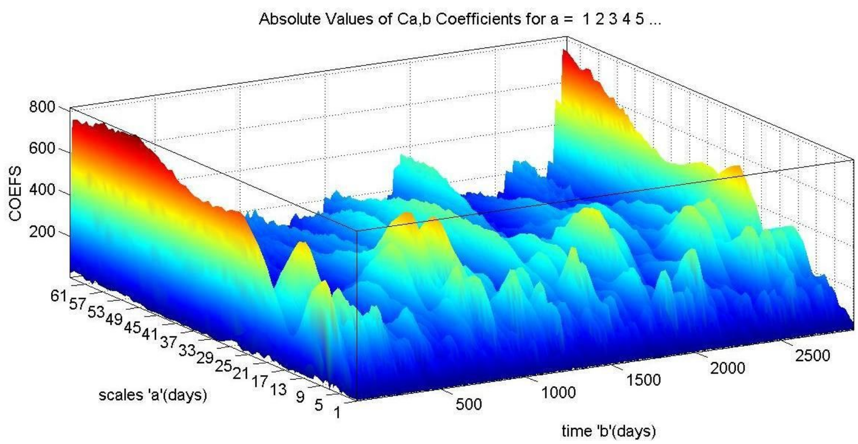

Figure 14: CWT periodogram of daily SW flow speed for solar cycle 24, revealing stationary and non-stationary periodic variations corresponding to 27, 13.5 and 9 days, while low frequency stationary noise shows up at Solar minima and nearby the Solar maxima

The stability of coronal holes may be inferred from the periodic variations of solar wind. The non-stationary 13.5-day and 9-day periodicity of solar wind speed arise due to the fast wind components, with speed more than 700 km/sec, the same being negligibly affected by the slow wind components. Our analysis shows that the 13.5-day and 9-day periodicities of solar wind speed at 1 AU arise because of the fast components of solar wind. Hence, the periodic breathing of Earth's atmosphere, having the same periodicity is evidently caused by the fast winds, and hence has direct relation with spatial distribution of coronal holes. As it can be seen, the periodicity of 13.5-day and 9-day occur only in the case of solar wind, but not in solar surface activity. From the wavelet power spectra, it is evident that in the 23rd cycle, 9-day periodicity occur throughout the 11-year cycle, whereas the 13.5-day periodicity was observed only in the declining phase of the cycles. This may refer to two types of coronal holes, one being present almost over the whole cycle, whereas the other type appears in the declining phase. Drawing the same inferences for the 24thcycle is not convincing, since till now we are only halfway through it. The 13.5-day periodicity has been claimed to be due to two active solar longitudes approximately 180^o apart, which occur around solar maxima [7] and have varying amplitudes in the two cycles. Similarly, the 9-day recurrence of fast solar wind streams originate from solar coronal holes distributed approximately 120^o apart in longitude, and further transmitting its affect on modulating the terrestrial environment as it hit Earth every 9 days [18]

4. CONCLUSION

In conclusion, the present analysis of the solar wind speed near 1 AU provides insight into the association of coronal holes, existing due to differential rotation and tilted axis of rotation of the Sun, with the solar wind. The solar wind variability has been examined for cycle 23 and 24. The periodic variations for the 24th cycle shows lower power, indicating less stationarity in the 24th cycle as compared to the 23rd cycle. It may be attributed to the fact that this 24th cycle is yet to reach the half-way mark**.** The wavelet transform reveals the non-stationarity of these periodic components, manifested as the fast components in the solar wind during the minima-maxima phase of the Solar cycle, which affects Earth's atmosphere. Thus, it is proved that the spatial variation of coronal holes has important effect on solar wind periodicity at 1 AU. The obtained 13.5-day periodicity in the wind speed is due to the combined effect of solar rotation and the appearance of coronal holes 180^o apart in longitude. In the global wavelet spectra of solar wind speed for both solar cycle 23 and 24, the 13.5-day periodicity can be observed, whose non-stationarity is dependent on the topological changes of these particular set of coronal holes. From this observation, we conclude that the appearance of 13.5-day period corresponds to the duration of appearance of the coronal holes, which has been possible to infer from an analysis of the wavelet spectra. In a similar manner, the 9-day period of solar wind can also be explained as a consequence of coronal holes situated at longitudes 120^o apart. From the context of fast wind being emanating from coronal holes and the dependence of solar wind speed periodicity with the location of coronal holes, an important inference can be drawn that lower periods of 13.5-day and 9-days arise due to the fast components of solar wind which eventually comes from the coronal holes. The implication of this understanding on terrestrial atmosphere needs to be studied further.

ACKNOWLEDGEMENT

MA expresses sincere gratitude to Dr. Eeshankur Saikia for valuable discussions and much needed support while carrying out the work as well as in the preparation of the manuscript. MA also thanks the Department of Physical Sciences, IISER Kolkata, for giving the opportunity to carry out a part of this work there.

REFERENCES

[1] J. L. Phillips, *Science,* p. 268, (1995).

[2] J. T. Gosling, S. Bame, D. J. McComas and J. L. Phillip, *Geophys. Res. Lett.,* vol. 17, p. 901, (1990).

[3] G. Poletto, *Journal of Advanced Research,* vol. 4, p. 215, (2013).

[4] U. Feldman, E. Landi, and N. A. Schwadron, *J. Geophys. Res.,* vol. 110, p. 2156, (2005).

[5] D. G. Cole, *Adv. Space Res.,* vol. 107, p. 295, (2003).

[6] R. Schwenn, *Living Rev. Solar Phys,* vol. 3, (2006).

[7] K. Mursula and B. Zieger, *J. Geophys. Res.,* vol. 101, (1996).

[8] S. K. Solanki, I. G. Usoskin, B. Kromer, M. Schussler and J. Beer, *Letters to Nature,* vol. 431, (2004).

[9] P. Janardhan, *J. Geophys. Res.,* vol. 120, (2015).

[10] J. P. Thayer, J. Lei, J. M. Forbes, E. K. Sutton and R. S. Nerem, *J. Geophys. Res.,* vol. 113, (2008).

[11] S. J. Schiff D. T. Kaplan T. Sauer P. So, E. Ott and C. Grebogi, *Phys. Rev. Lett.,* vol. 76, (1996).

[12] K. C. S. Bochner, Fourier Transforms, Princeton University Press, (1949).

[13] B. B. Hubbard, The World According to Wavelets, Wellesley, Massachusetts: AK Peters, (1997).

[14] I. Daubechies, "Ten lectures on wavelets," in *CBMS-NSF Regional Conference Series in Applied Mathematics*, Philadelphia, (1992).

[15] M. Akay, Time Frequency and Wavelets in Biomedical Signal Processing, Wiley-IEEE Press, (1997).

[16] C. T. a. G. P. Compo, *Bulletin of the American Meteorological Society,* vol. 79, p. 61, (1998).

[17] A. Kavanagh and M. Denton, *Astronomy and Geophysics,* vol. 48, p. 6.24, (2007).

[18] J. Lei, J. P. Thayer, J. M. Forbes, E. K. Sutton, R. S. Nerem, *Geophys. Res. Lett.,* vol. 35, (2008).